

Selective multiphoton ionization of sodium by femtosecond laser pulses

A. Bunjac, D. B. Popović and N. S. Simonović

Institute of Physics, University of Belgrade, Pregrevica 118, 11080 Belgrade, Serbia

1. Introduction

Freeman et al. (1987) have shown that when atomic states during the laser pulse transiently shift into resonance due to the dynamic (or AC) Stark shift, the resonantly enhanced multiphoton ionization (REMPI) takes place, increasing the photoelectron yield, and one observes peaks at the corresponding values of photoelectron energy. Thus, the peaks in the PES are related to the REMPI occurring via different intermediate states.

A particular challenge is the selective ionization of the atom through a single energy level which could produce a high ion yield. Hart et al (2016) have shown that such a process could be achieved by controlling the resonant dynamic Stark shift of sodium states via intensity of the laser pulse of an appropriate wavelength.

Here we study the multiphoton ionization (MPI) of the sodium atom by the laser pulse of 800 nm wavelength and 57 fs full width at half maximum (FWHM) with the peak intensities ranging from 3.5 to 8.8 TW/cm², which are the same values as used in the experiment by Hart et al.

2. Model, Energy Scheme and Photoionization Channels

Within the single-electron model the dynamics of the valence (active) electron of sodium atom in an alternating electric field $F(t)$ is described by Hamiltonian (in atomic units)

$$H = \frac{\mathbf{p}^2}{2} + V_{\text{core}}(r) - F(t)z. \quad (1)$$

The effective core potential $V_{\text{core}}(r)$ describes the interaction of the valence electron with the atomic core (inner electrons + atomic nucleus). For this purpose we use the Hellmann's pseudopotential $V_{\text{core}}(r) = -1/r + Ae^{-ar}/r$. The parameters $A = 21$ and $a = 2.54920$ provide the correct value for the ionization potential of lithium $I_p = 5.1391 \text{ eV} = 0.18886 \text{ a.u.}$ and reproduce approximately the energies of singly-excited states (see Fig. 1).

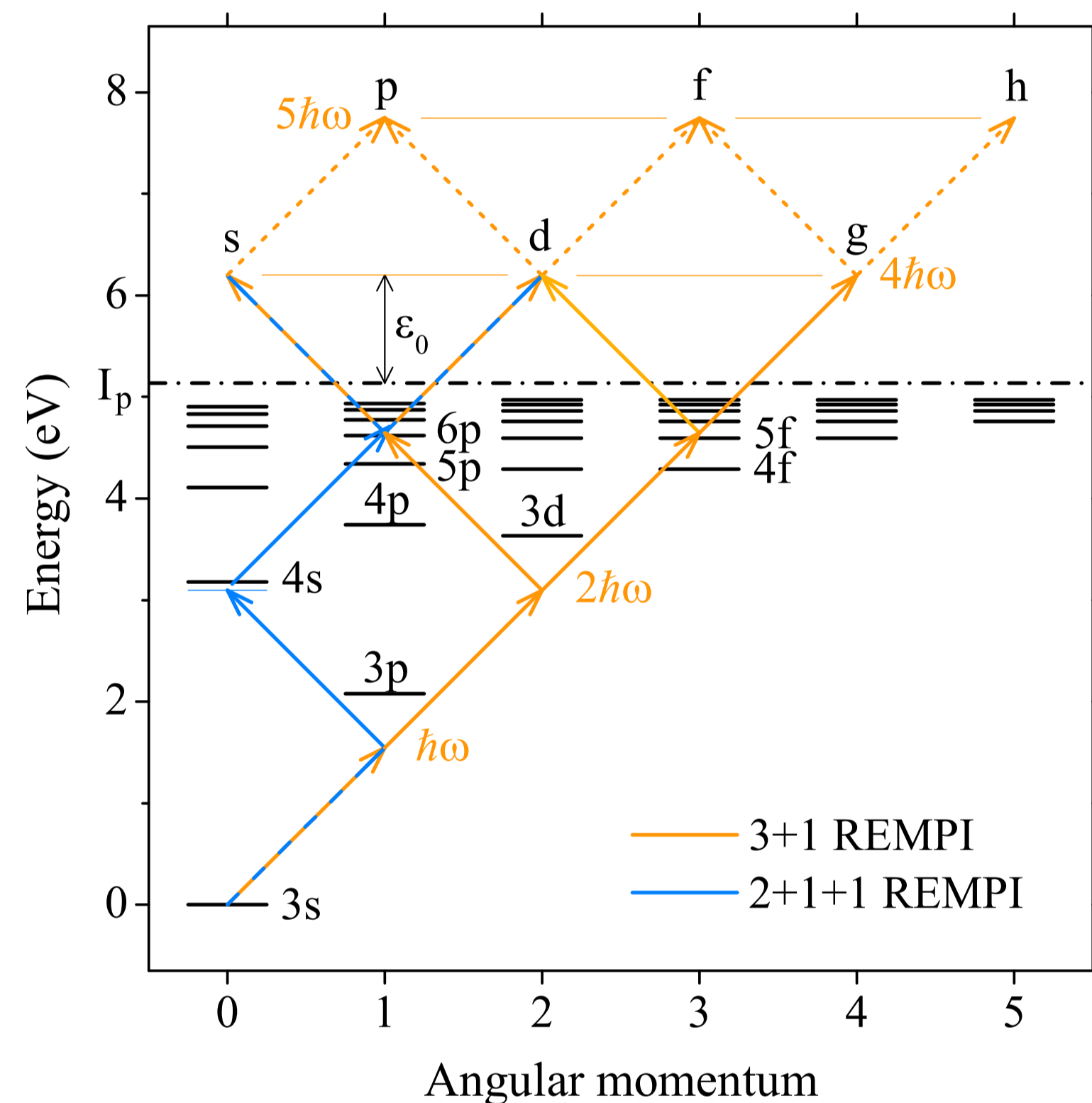


Figure 1. The unperturbed energy levels (short black lines) corresponding to singly excited states of sodium relative to its ground state (3s) and possible four-photon and five-photon absorption pathways (arrows) from the ground state to continuum for the radiation of 800 nm wavelength ($\hbar\omega \approx 1.55 \text{ eV}$). The continuum boundary is drawn by the dash-dot line and ϵ_0 is the excess energy of photoelectrons produced in the nonresonant four-photon ionization.

We consider a linearly polarized laser pulse of the form

$$F(t) = F_{\text{peak}} \sin^2(\pi t/T_p) \cos(\omega t), \quad 0 < t < T_p \quad (2)$$

(otherwise $F(t) = 0$). Here ω , F_{peak} and T_p are the frequency of laser field, the peak value of its electric component and the pulse duration ($2 \times \text{FWHM}$), respectively. Due to the axial symmetry of the system, the magnetic quantum number m of the valence electron is a good quantum number and we set $m = 0$ (the ground state value).

The photoionization process is simulated by calculating the evolution of the wave function of valence electron $\psi(\mathbf{r}, t)$, which is initially ($t = 0$) chosen to be the lowest eigenstate of Hamiltonian (1) (then $F = 0$) that describes the sodium ground state. The evolution is calculated by integrating the TDSE (see Bunjac et al., 2017).

Fig. 1(a) shows the lowest energy levels corresponding to singly-excited states of sodium and possible multiphoton absorption pathways during the interaction of the atom with a laser radiation of 800 nm wavelength ($\hbar\omega = 0.05695 \text{ a.u.} \approx 1.55 \text{ eV}$). At this wavelength there are three dominant REMPI channels:

- (i) (3+1)-photon ionization via excitation of 5p, 6p and 7p states, giving rise to photoelectrons with s and d-symmetry;
- (ii) (3+1)-photon ionization via excitation of 4f, 5f and 6f states, producing photoelectrons with d and g-symmetry;
- (iii) (3+1+1)-photon ionization via nearly resonant two-photon transition $3s \rightarrow 4s$ and subsequent excitation of P-states, giving rise to photoelectrons with s and d-symmetry.

3. Partial wave analysis

In order to determine the photoelectron energy spectrum (PES), the outgoing part of the active electron wave function $\psi(\mathbf{r}, t)$ at a time $t > T_p$ is transformed from the coordinate to momentum representation $\bar{\psi}(\mathbf{k}, t)$ by the Fourier transform and expanded in terms of partial waves

$$\bar{\psi}(\mathbf{k}) = \sum_l \Phi_l(k) Y_{l0}(\vartheta), \quad (3)$$

where $Y_{l0}(\vartheta)$ are the spherical harmonics with $m = 0$ and $\Phi_l(k) = \int Y_{l0}^*(\vartheta) \bar{\psi}(\mathbf{k}) d\Omega$ are the corresponding radial functions. Using the representation of $\bar{\psi}$ in cylindrical coordinates, the radial functions can be calculated as

$$\Phi_l(k) = 2\pi \int_0^\pi \bar{\psi}(k \sin \vartheta, k \cos \vartheta) Y_{l0}(\vartheta) \sin \vartheta d\vartheta. \quad (4)$$

According to partial wave expansion (3), the radial probability density of photoelectrons in momentum space is the sum $w(k) = \sum_l w_l(k)$, where

$$w_l(k) = |\Phi_l(k)|^2 k^2 \quad (5)$$

are the partial probability densities. These quantities for $l = 0, \dots, 5$, as functions of the photoelectron excess energy $\epsilon = \hbar^2 k^2 / 2m_e$, are shown in the left column of Fig. 2 for three values of the laser peak intensity: 3.5, 4.9 and 8.8 TW/cm². The corresponding total probability densities w represent the PES for these three values of laser intensity. They are shown in the right column of Fig. 2 together with the corresponding spectra obtained experimentally (Hart et al., 2016).

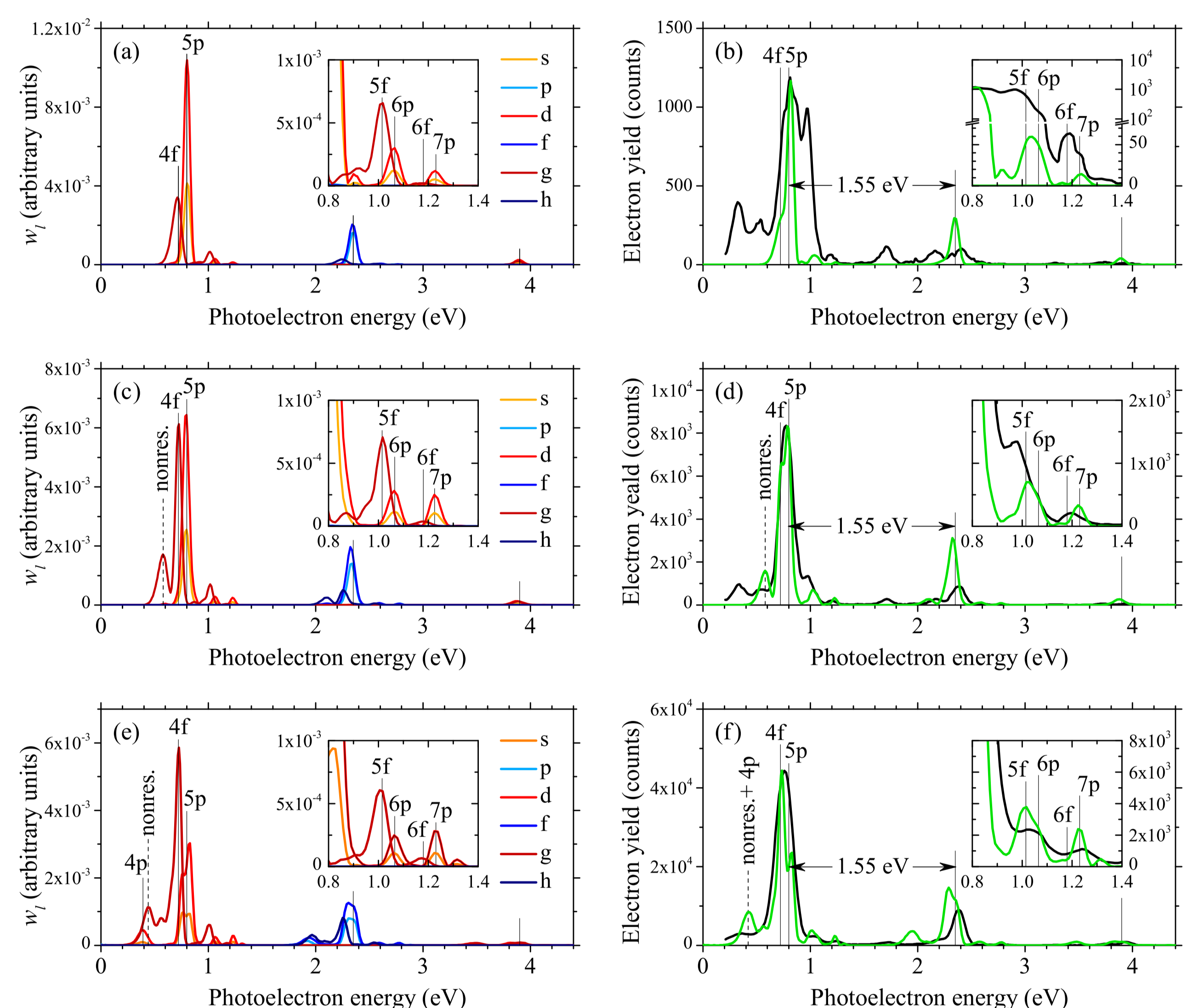


Figure 2. Partial probability densities w_l for $l = 0, \dots, 5$ (left column) and the total probability density w (right column, green line) as functions of the photoelectron energy $\epsilon = \hbar^2 k^2 / (2m_e)$ obtained at three values of the laser peak intensity: (a,b) 3.5 TW/cm², (c,d) 4.9 TW/cm², (e,f) 8.8 TW/cm². Experimental results (Hart et al., 2016) are represented by full black lines. The full vertical lines mark the energies of two REMPI channels (via f and p states) of the threshold peak as well as the position of 5p subpeak in the higher order ATI peaks.

The spectra, both the calculated and experimental, exhibit a typical above threshold ionization (ATI) structure with prominent peaks separated by the photon energy $\hbar\omega \approx 1.55 \text{ eV}$. Fig. 2 shows the peaks corresponding to lowest three orders of ATI (MPI by 4 + s photons, $s = 0, 1, 2$) which are located approximately at $\epsilon = 0.8 \text{ eV} + s\hbar\omega$.

The partial wave analysis recovers the character of ATI peaks. We see in Fig. ?? (left) that for the photoelectron energies around the main peak ($s = 0$, $\epsilon \approx 0.8 \text{ eV}$) and around the second-order ATI peak ($s = 2$, $\epsilon \approx 3.9 \text{ eV}$) dominant contributions in the total probability density come from the partial waves with even l (s, d, g-waves). Thus, the photoelectrons with these energies are generated by absorbing an even number of photons ($N = 4$ and 6). Contrarily, in the vicinity of the first-order ATI peak ($s = 1$, $\epsilon \approx 2.35 \text{ eV}$) the partial waves with even l are suppressed and those with odd l (p, f, h-waves) dominate. Therefore, in this case odd number of photons is absorbed (here $N = 5$).

Fig. 2 (left column) shows that at the laser peak intensity of 3.5 TW/cm² dominant contribution in the main peak (around 0.8 eV) comes from d-electrons, while at the intensity of 8.8 TW/cm² the electrons of g-symmetry dominate. In conclusion, by changing the laser intensity, one selects the main ionization channel – in the first case this is the 3+1 (or 2+1+1) REMPI via 5p state, while in the second case it is the 3+1 REMPI via 4f state.

References

- A. Bunjac, D. B. Popović and N. S. Simonović, *Phys. Chem. Chem. Phys.*, **19**, 19829 (2017).
 R. R. Freeman, P. H. Bucksbaum, H. Milchberg, S. Darack, D. Schumacher and M. E. Geusic, *Phys. Rev. Lett.*, **59**, 1092 (1987).
 N. A. Hart, J. Strohaber, A. A. Kolomenskii, G. G. Paulus, D. Bauer and H. A. Schuessler, *Phys. Rev. A* **93**, 063426 (2016).